

## Chapter 4

### Results



## Mechanical Testing Results

### 1. Tensile Testing

Table 4.1.1 and 4.1.2 shows the tensile properties of the composites at crosshead speed of 0.5 and 1.0 mm min<sup>-1</sup>, respectively. The stress-strain behaviour of all specimens are shown at Appendix and some examples of these are shown in Fig.4.1.1 and 4.1.2. The stress-strain curves of calcined bone ash reinforced polyethylene composites at various volume fraction are summarized in Fig.4.1.3 and 4.1.4. In addition the variation of Young's modulus, tensile strength, strain to failure, energy to failure and toughness for various volume fraction of calcined bone ash and synthetic hydroxyapatite reinforced polyethylene composites are shown in Fig.4.1.5, 4.1.6, 4.1.7, 4.1.8 and 4.1.9., respectively. Also, Fig.4.1.10 and 4.1.11 represents effect of cross-head speed to Young's modulus and tensile strength of calcined bone ash reinforced polyethylene composite.

The results indicated that the elastic modulus increased with increased filler loading but the strain to failure decreased at the same time. The tensile strength remained stable at high concentration of filler.

Table 4.1.1 Tensile properties of calcined bone ash and synthetic hydroxyapatite reinforced high density polyethylene composites as a function of volume fraction of filler at crosshead speed of 0.5 mm min<sup>-1</sup>. (\* = one specimen)

Property	Volume fraction	Young's modulus	Tensile strength	Strain to failure	Energy to failure	Toughness
Materials	V <sub>f</sub>	GPa	MPa	%	J	MPa
HDPE*	0	0.81	24.78	102.53	19.36	23.18
CBA	0.20	1.62 ± 0.16	22.22 ± 0.48	41.92 ± 1.56	7.39 ± 0.44	8.79 ± 0.46
	0.30	2.42 ± 0.06	20.02 ± 0.67	22.90 ± 0.66	3.55 ± 0.36	4.59 ± 0.19
	0.35	2.82 ± 0.08	21.41 ± 0.18	20.28 ± 2.45	3.26 ± 0.54	4.04 ± 0.51
	0.45	4.23 ± 0.10	22.28 ± 0.27	1.72 ± 0.09	0.42 ± 0.06	0.46 ± 0.04
	*	0.50	4.33	22.33	0.85	0.09
Syn. HA	0.20	1.80 ± 0.19	26.14 ± 0.50	21.75 ± 4.56	4.21 ± 0.95	5.17 ± 1.09
	0.35	3.38 ± 0.06	22.25 ± 1.35	7.79 ± 2.06	1.37 ± 0.35	1.63 ± 0.52



Table 4.1.1 Tensile properties of calcined bone ash and synthetic hydroxyapatite reinforced high density polyethylene composites as a function of volume fraction of filler at crosshead speed of 0.5 mm min<sup>-1</sup>. (\* = one specimen)

Property	Volume fraction	Young's modulus GPa	Tensile strength MPa	Strain to failure %	Energy to failure J	Toughness MPa
Materials	V <sub>f</sub>					
HDPE*	0	0.81	24.78	102.53	19.36	23.18
CBA	0.20	1.62 ± 0.16	22.22 ± 0.48	41.92 ± 1.56	7.39 ± 0.44	8.79 ± 0.46
	0.30	2.42 ± 0.06	20.02 ± 0.67	22.90 ± 0.66	3.55 ± 0.36	4.59 ± 0.19
	0.35	2.82 ± 0.08	21.41 ± 0.18	20.28 ± 2.45	3.26 ± 0.54	4.04 ± 0.51
	0.45	4.23 ± 0.10	22.28 ± 0.27	1.72 ± 0.09	0.42 ± 0.06	0.46 ± 0.04
	*	0.50	4.33	22.33	0.85	0.09
Syn. HA	0.20	1.80 ± 0.19	26.14 ± 0.50	21.75 ± 4.56	4.21 ± 0.95	5.17 ± 1.09
	0.35	3.38 ± 0.06	22.25 ± 1.35	7.79 ± 2.06	1.37 ± 0.35	1.63 ± 0.52

Table 4.1.1 Tensile properties of calcined bone ash and synthetic hydroxyapatite reinforced high density polyethylene composites as a function of volume fraction of filler at crosshead speed of  $0.5 \text{ mm min}^{-1}$ . (\* = one specimen)

Property	Volume fraction	Young's modulus GPa	Tensile strength MPa	Strain to failure %	Energy to failure J	Toughness MPa
Materials	$V_f$					
HDPE*	0	0.81	24.78	102.53	19.36	23.18
CBA	0.20	$1.62 \pm 0.16$	$22.22 \pm 0.48$	$41.92 \pm 1.56$	$7.39 \pm 0.44$	$8.79 \pm 0.46$
	0.30	$2.42 \pm 0.06$	$20.02 \pm 0.67$	$22.90 \pm 0.66$	$3.55 \pm 0.36$	$4.59 \pm 0.19$
	0.35	$2.82 \pm 0.08$	$21.41 \pm 0.18$	$20.28 \pm 2.45$	$3.26 \pm 0.54$	$4.04 \pm 0.51$
	0.45	$4.23 \pm 0.10$	$22.28 \pm 0.27$	$1.72 \pm 0.09$	$0.42 \pm 0.06$	$0.46 \pm 0.04$
	*	0.50	4.33	22.33	0.85	0.09
Syn. HA	0.20	$1.80 \pm 0.19$	$26.14 \pm 0.50$	$21.75 \pm 4.56$	$4.21 \pm 0.95$	$5.17 \pm 1.09$
	0.35	$3.38 \pm 0.06$	$22.25 \pm 1.35$	$7.79 \pm 2.06$	$1.37 \pm 0.35$	$1.63 \pm 0.52$

Table 4.1.1 Tensile properties of calcined bone ash and synthetic hydroxyapatite reinforced high density polyethylene composites as a function of volume fraction of filler at crosshead speed of 0.5 mm min<sup>-1</sup>. (\* = one specimen)

Property	Volume fraction	Young's modulus GPa	Tensile strength MPa	Strain to failure %	Energy to failure J	Toughness MPa
Materials	V <sub>f</sub>					
HDPE*	0	0.81	24.78	102.53	19.36	23.18
CBA	0.20	1.62 ± 0.16	22.22 ± 0.48	41.92 ± 1.56	7.39 ± 0.44	8.79 ± 0.46
	0.30	2.42 ± 0.06	20.02 ± 0.67	22.90 ± 0.66	3.55 ± 0.36	4.59 ± 0.19
	0.35	2.82 ± 0.08	21.41 ± 0.18	20.28 ± 2.45	3.26 ± 0.54	4.04 ± 0.51
	0.45	4.23 ± 0.10	22.28 ± 0.27	1.72 ± 0.09	0.42 ± 0.06	0.46 ± 0.04
	*	0.50	4.33	22.33	0.85	0.09
Syn. HA	0.20	1.80 ± 0.19	26.14 ± 0.50	21.75 ± 4.56	4.21 ± 0.95	5.17 ± 1.09
	0.35	3.38 ± 0.06	22.25 ± 1.35	7.79 ± 2.06	1.37 ± 0.35	1.63 ± 0.52

Table 4.1.2 Tensile properties of calcined bone ash and synthetic hydroxyapatite reinforced high density polyethylene composites as a function of volume fraction of filler at crosshead speed of 1.0 mm min<sup>-1</sup>. (\* = one specimen)

Property	Volume fraction	Young's modulus GPa	Tensile strength MPa	Strain to failure %	Energy to failure J	Toughness MPa
Materials	V <sub>f</sub>					
HDPE*	0	14.73	24.46	54.09	4.27	11.94
CBA	0.20	13.59 ± 1.45	20.88 ± 0.73	49.77 ± 0.16	3.57 ± 0.09	9.95 ± 0.58
	0.30	14.51 ± 1.21	20.87 ± 1.36	24.79 ± 3.33	1.83 ± 0.34	5.00 ± 0.91
	0.35	16.39 ± 3.53	17.72 ± 0.98	21.79 ± 5.68	1.32 ± 0.23	3.75 ± 0.61
	0.45	20.90 ± 7.48	21.51 ± 0.23	7.46 ± 2.13	0.57 ± 0.16	1.55 ± 0.46
*	0.50	29.24	19.75	0.04	0.001	0.003
Syn. HA	0.20	13.22 ± 0.54	25.44 ± 0.32	24.59 ± 1.13	2.08 ± 0.08	5.94 ± 0.24
	0.35	20.75 ± 6.20	22.22 ± 0.37	11.02 ± 4.11	0.85 ± 0.31	2.38 ± 0.86

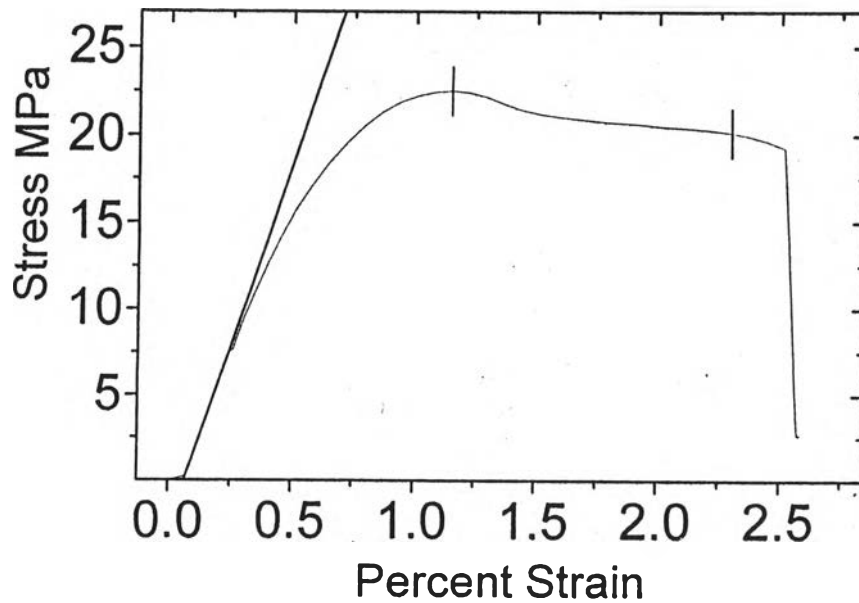


Figure 4.1.1 Stress-strain curve of calcined bone ash reinforced polyethylene composite at 0.45 volume fraction at crosshead speed of  $0.5 \text{ mm min}^{-1}$ .

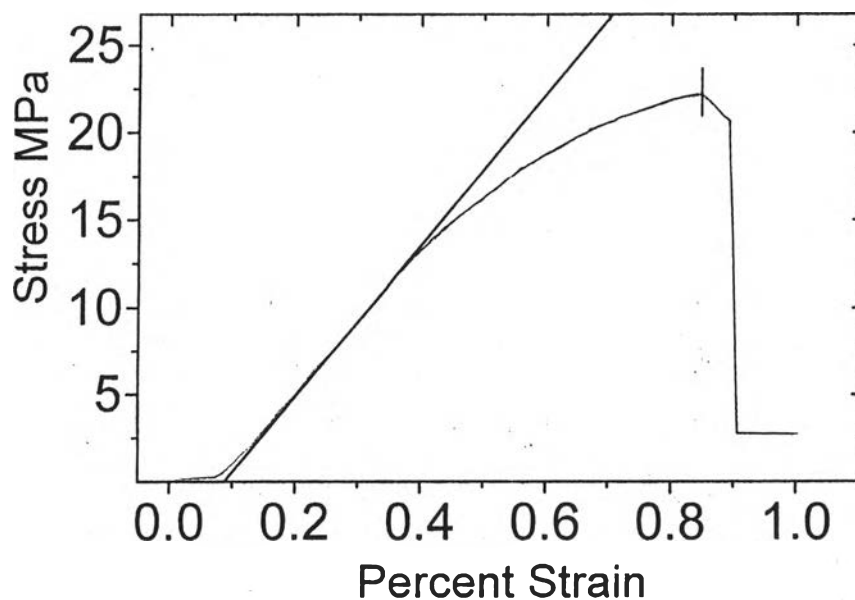


Figure 4.1.2 Stress-strain curve of calcined bone ash reinforced polyethylene composite at 0.50 volume fraction at crosshead speed of  $0.5 \text{ mm min}^{-1}$ .

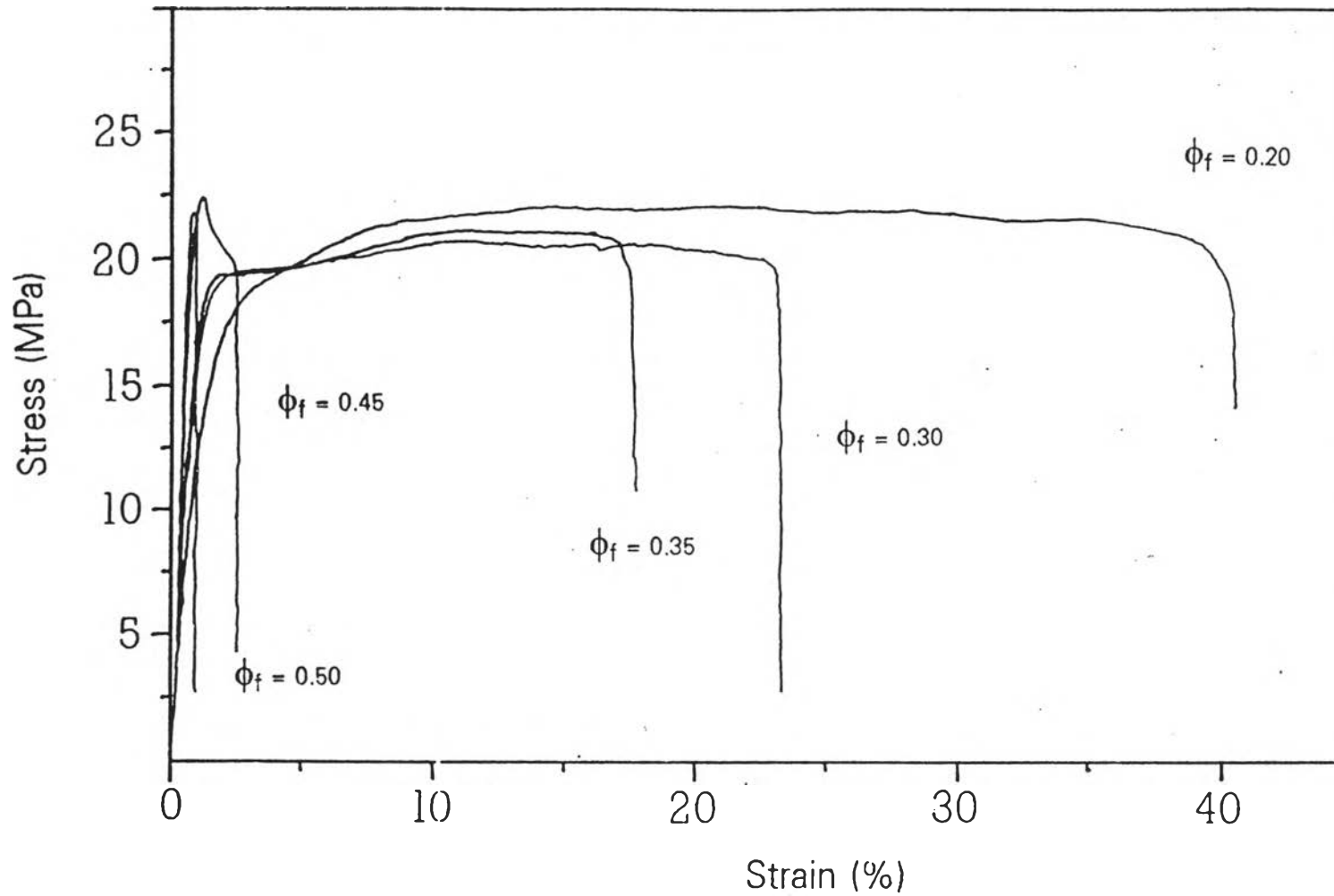


Figure 4.1.3 Stress-strain curves of calcined bone ash reinforced polyethylene composites at various volume fraction at crosshead speed of  $0.5 \text{ mm min}^{-1}$ .



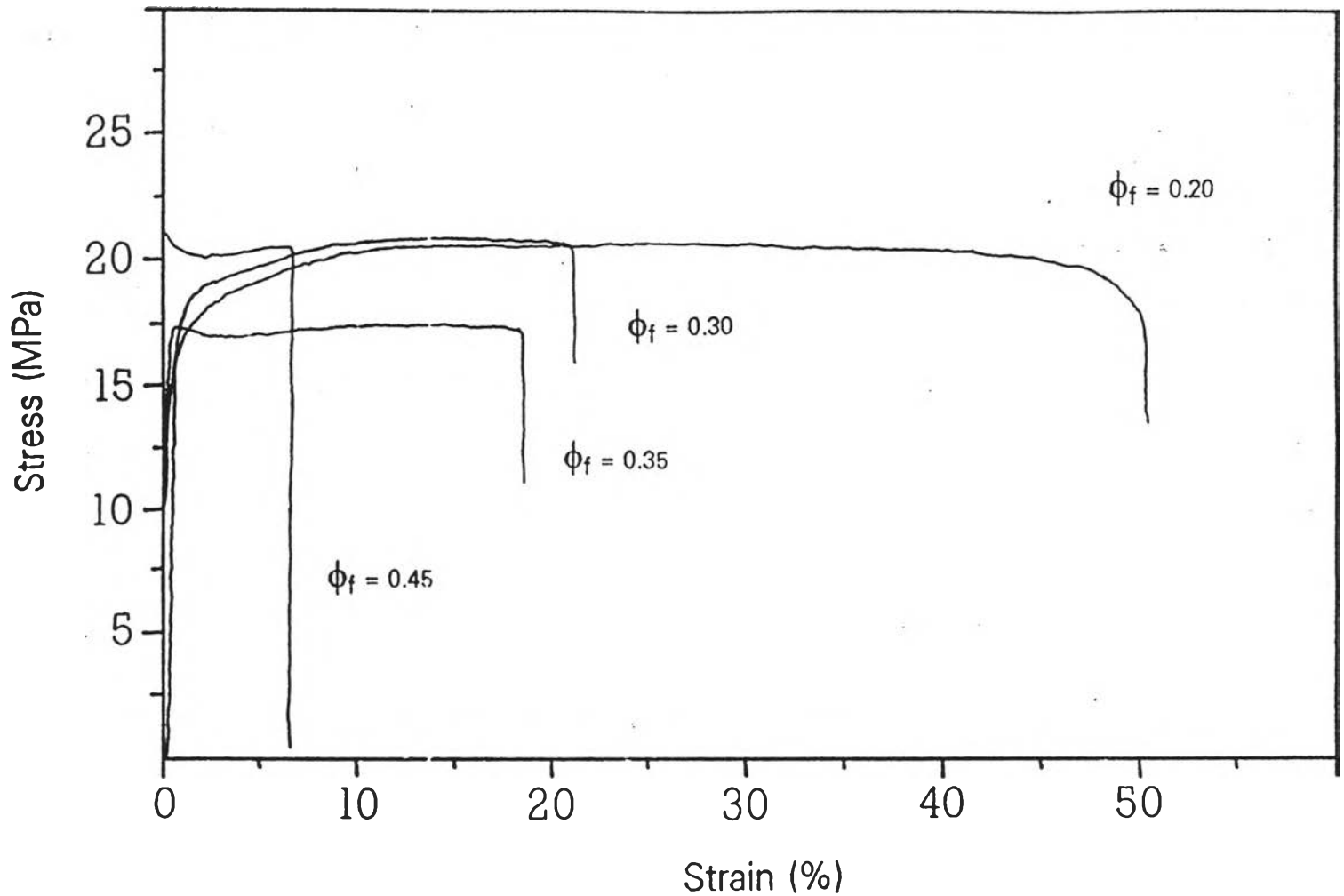


Figure 4.1.4 Stress-strain curves of calcined bone ash reinforced polyethylene composites at various volume fraction at crosshead speed of 1.0 mm min<sup>-1</sup>.

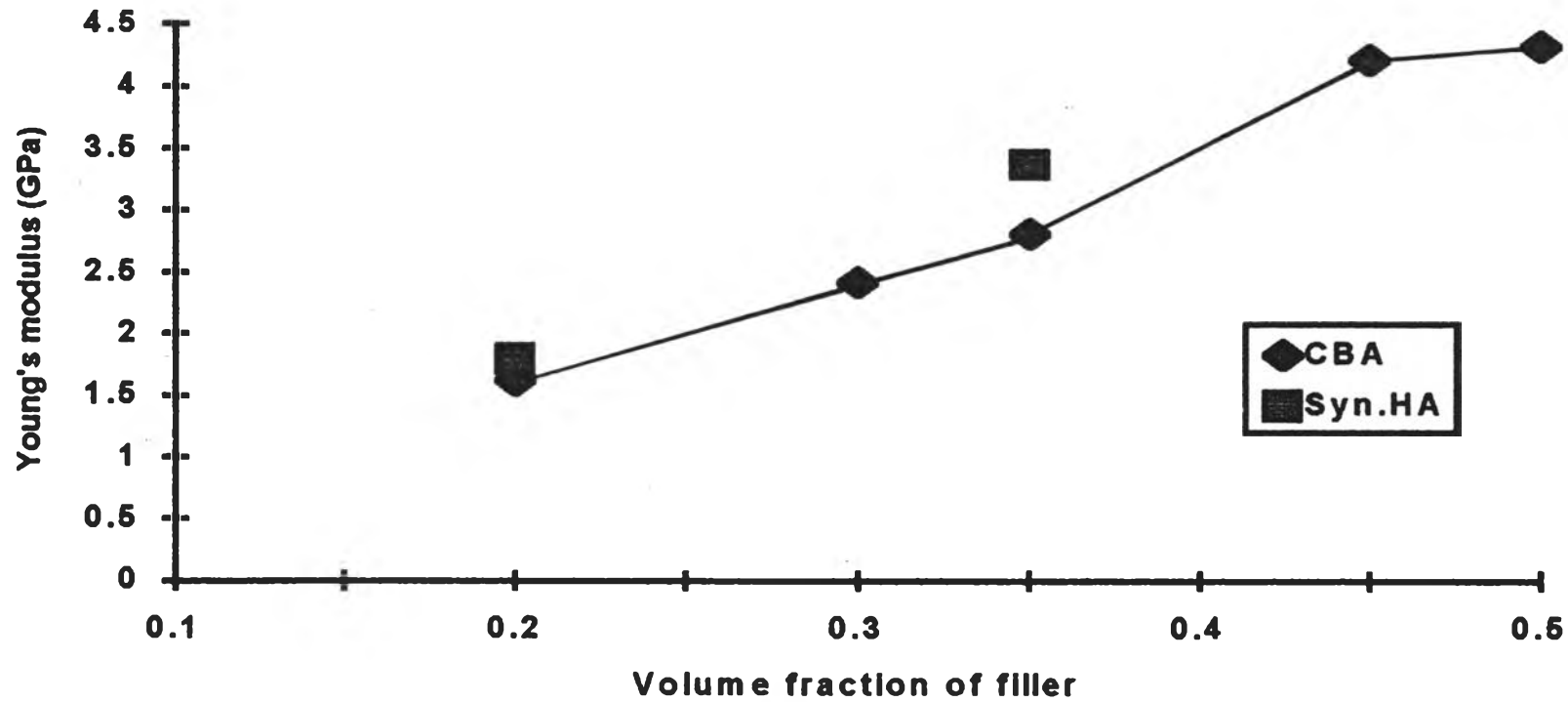


Figure 4.1.5 Young's modulus for various volume fraction of calcined bone ash and synthetic hydroxyapatite reinforced polyethylene composites at crosshead speed of  $0.5 \text{ mm min}^{-1}$ .

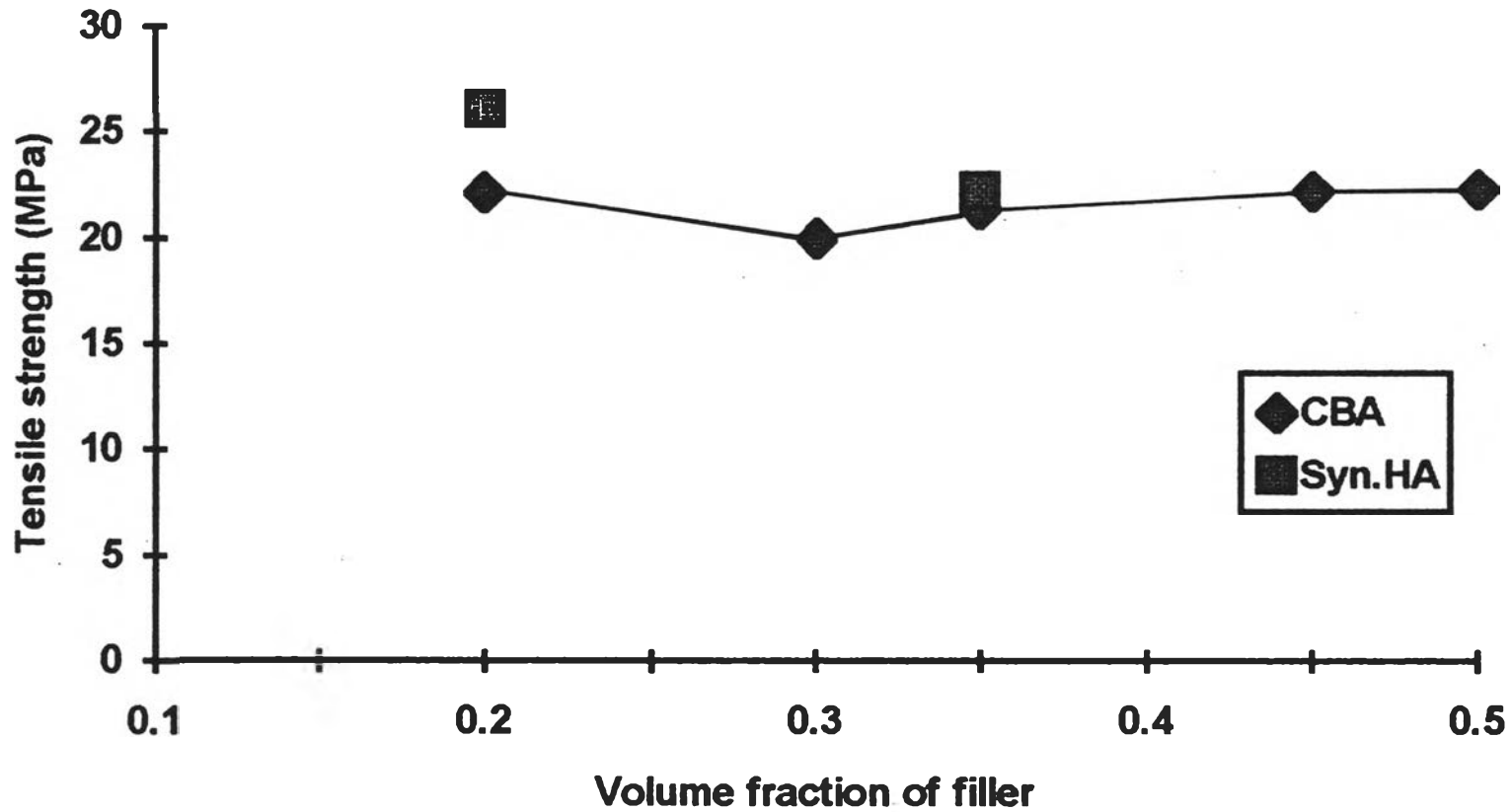


Figure 4.1.6 Tensile strength for various volume fraction of calcined bone ash and synthetic hydroxyapatite reinforced polyethylene composites at crosshead speed of  $0.5 \text{ mm min}^{-1}$ .

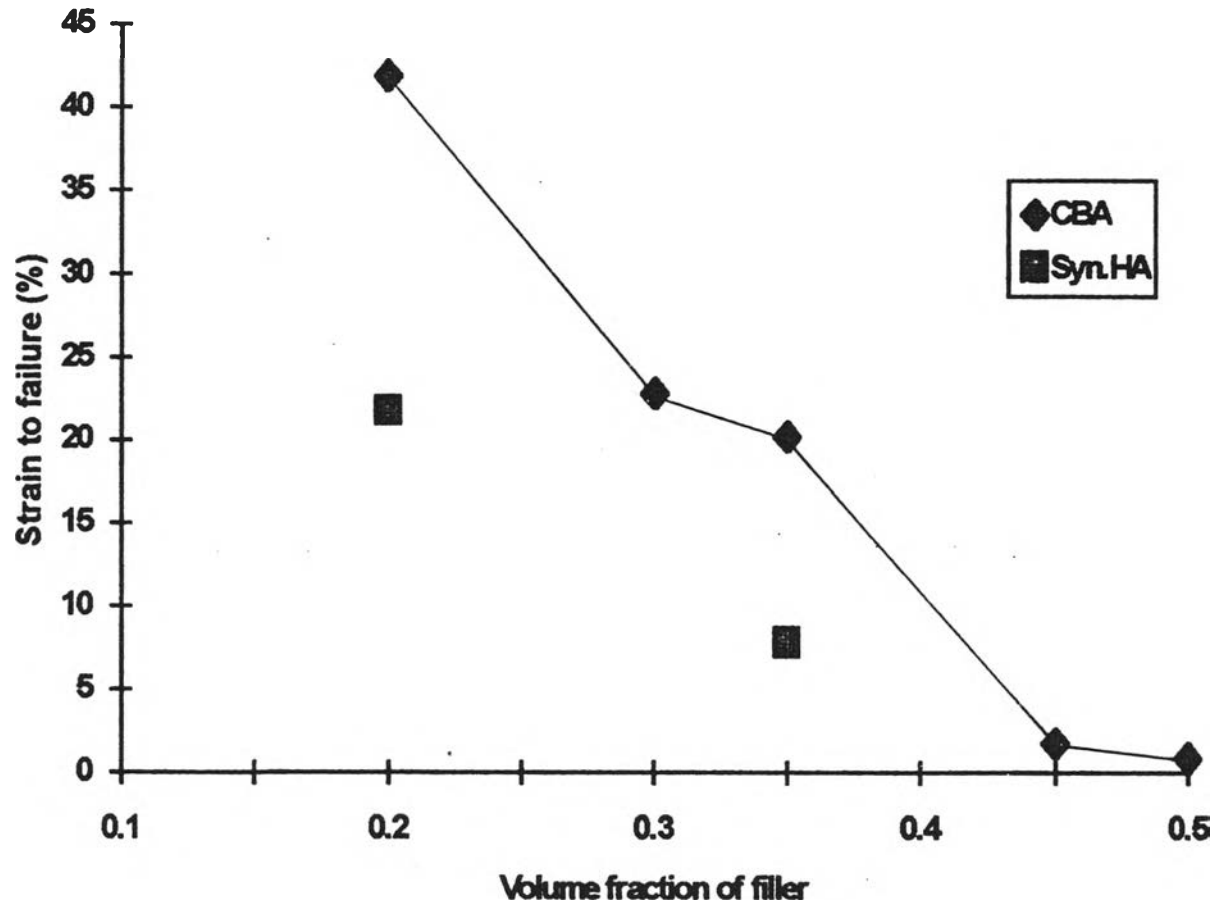


Figure 4.1.7 Strain to failure for various volume fraction of calcined bone ash and synthetic hydroxyapatite reinforced polyethylene composites at crosshead speed of  $0.5 \text{ mm min}^{-1}$ .

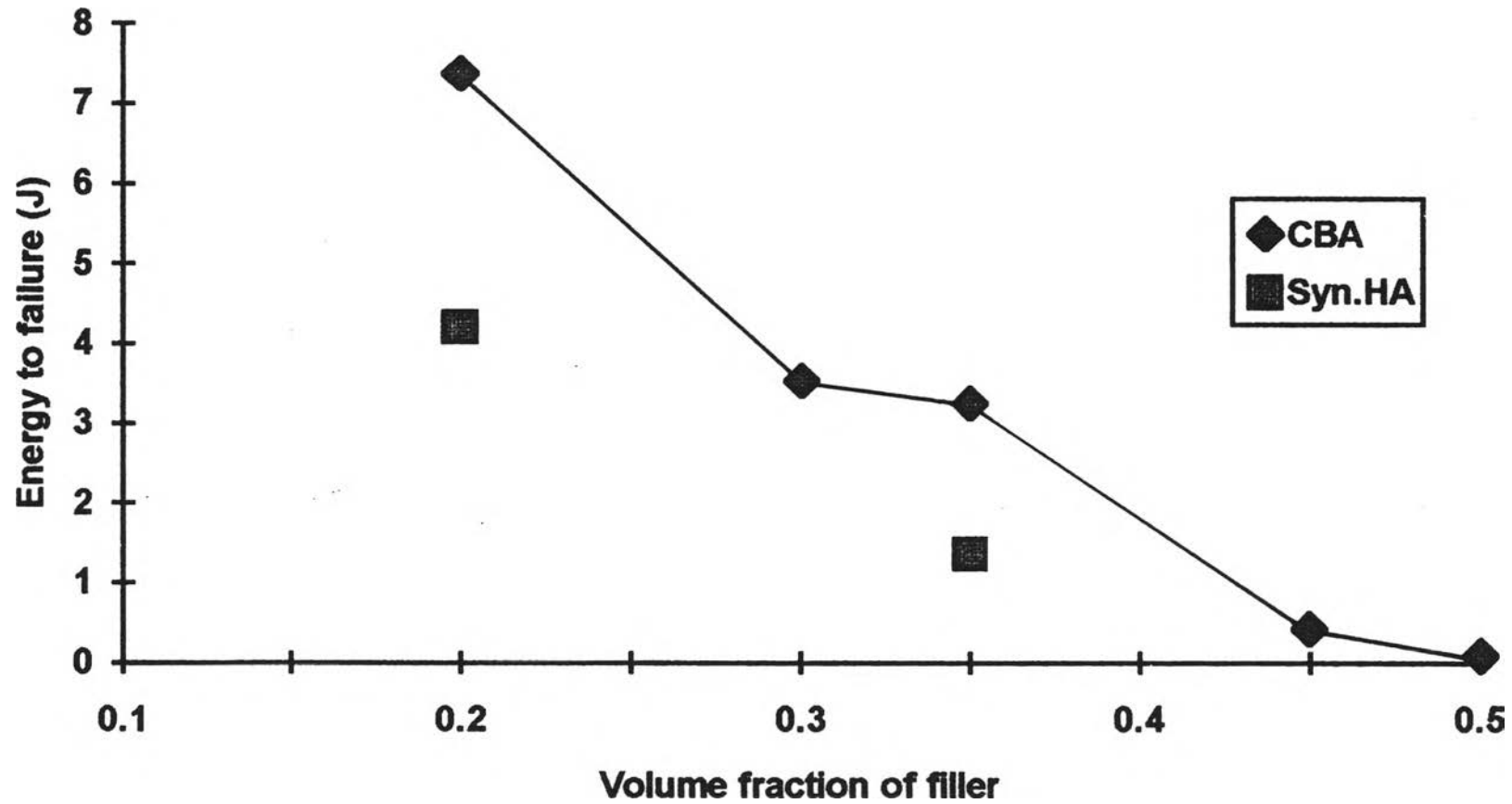


Figure 4.1.8 Energy to failure for various volume fraction of calcined bone ash and synthetic hydroxyapatite reinforced polyethylene composites at crosshead speed of  $0.5 \text{ mm min}^{-1}$ .

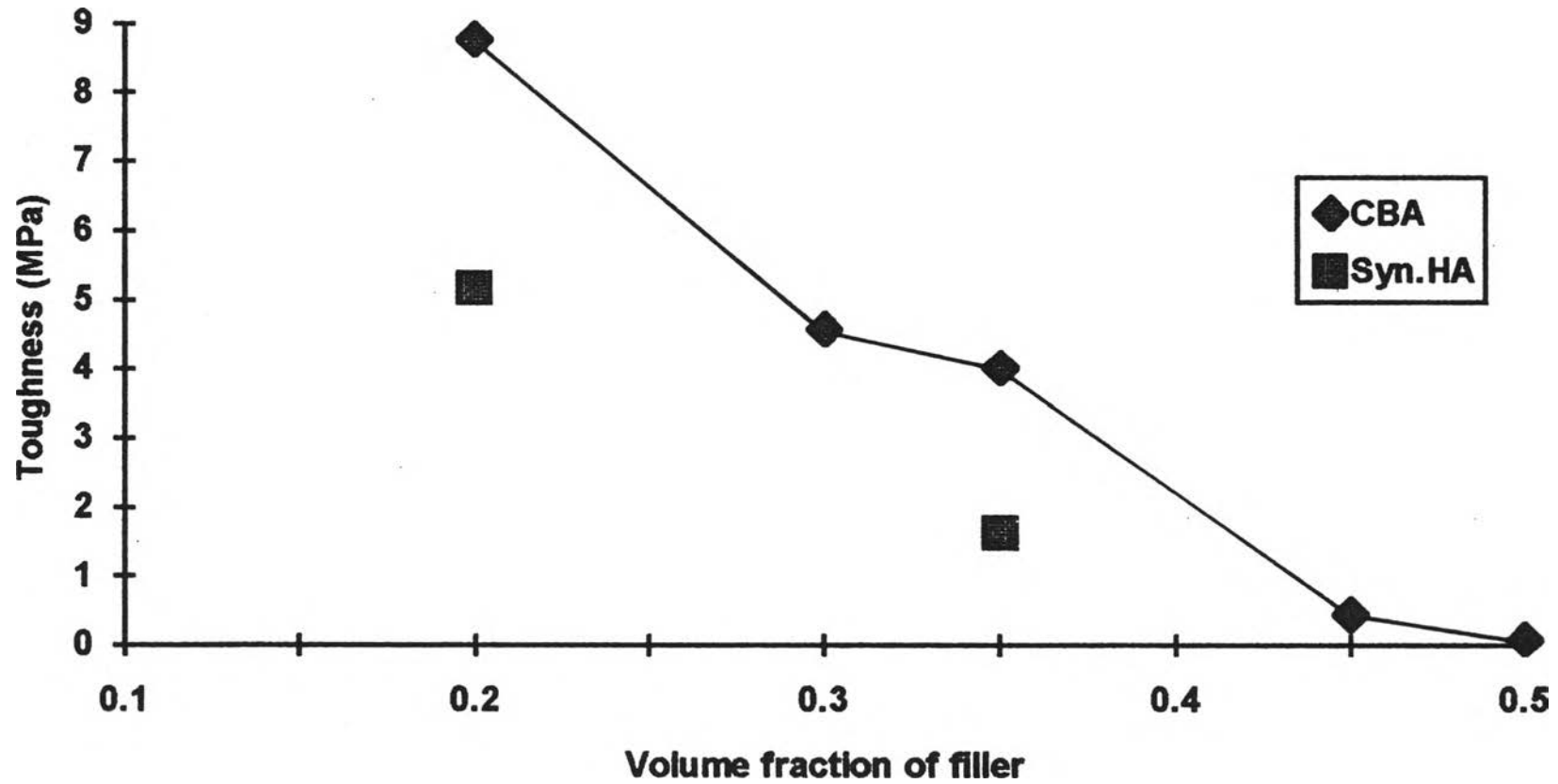


Figure 4.1.9 Toughness for various volume fraction of calcined bone ash and synthetic hydroxyapatite reinforced polyethylene composites at crosshead speed of  $0.5 \text{ mm min}^{-1}$ .

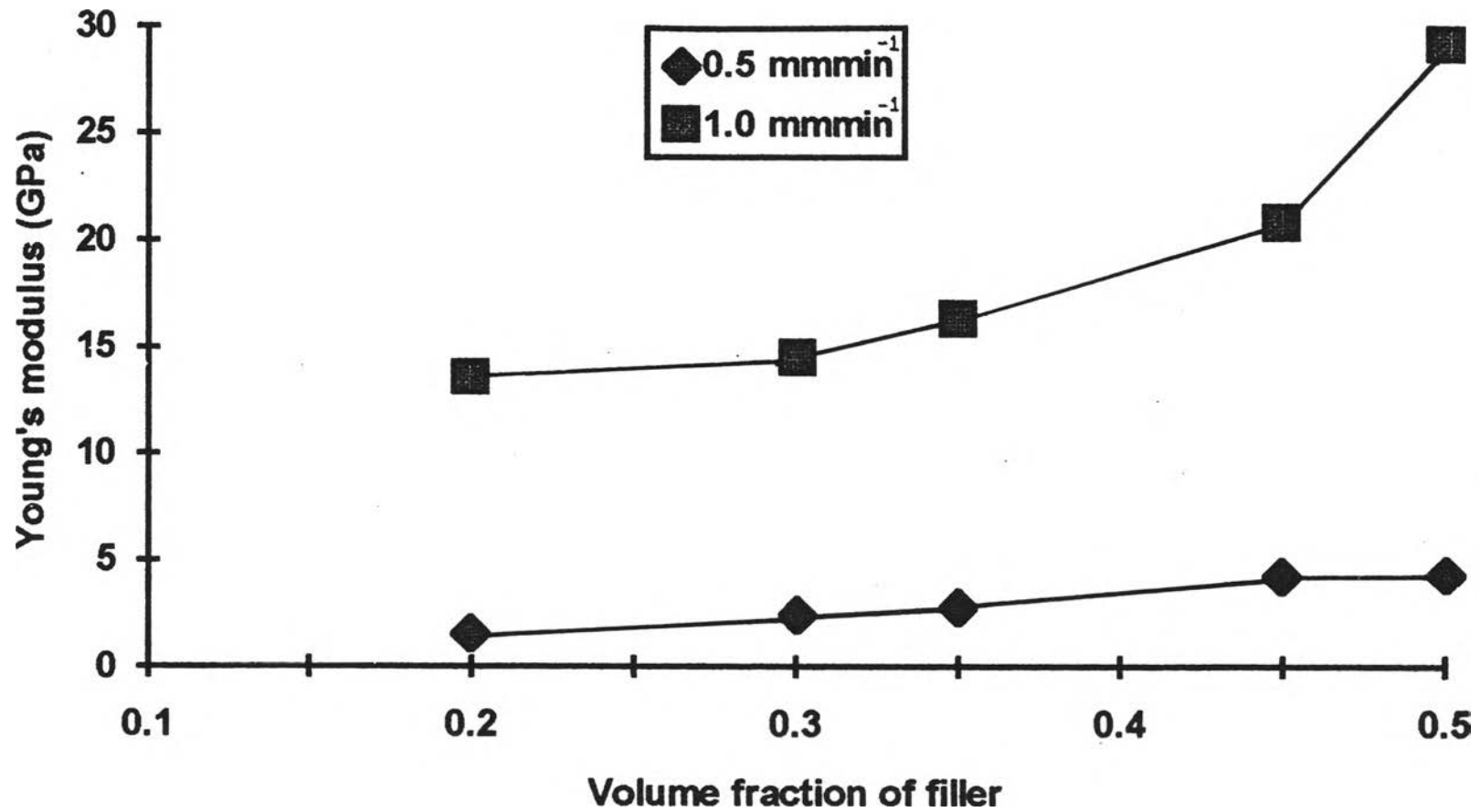


Figure 4.1.10 The effect of crosshead speed against Young's modulus for calcined bone ash reinforced polyethylene composites.

## 2. Flexural testing

The specimens below 0.45 volume fraction of calcined bone ash do not break at the specific strain limit, so flexural results can not be obtained. This is the threshold for brittle characteristic of the composites.

Table 4.1.3 Flexural results of 0.45 volume fraction of calcined bone ash reinforced polyethylene composite.

Flexural strength (MPa)	$26.79 \pm 1.80$
Flexural modulus (GPa)	$1.85 \pm 0.23$
Energy to yield point (J)	$0.03 \pm 0.01$

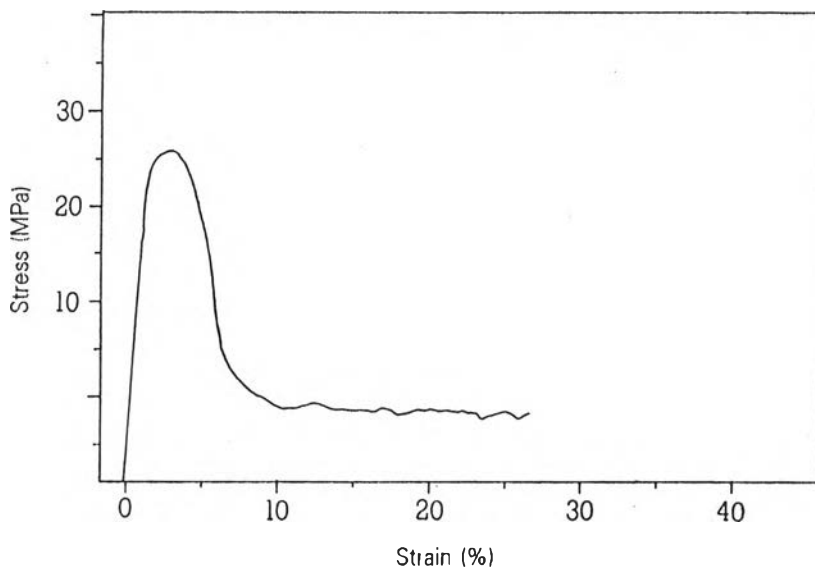


Figure 4.1.11 Stress-strain curve of flexural test for 0.45 volume fraction of calcined bone ash reinforced polyethylene composite.



### 3. Hardness

Table 4.1.4 Microhardness results of calcined bone ash and synthetic hydroxyapatite reinforced high density polyethylene composites.

Kinds	Volume fraction of filler	Vicker Hardness Number (VHN)
CBA	0.10	not display pyramid shape
	0.20	6.538 ± 0.586
	0.25	7.060 ± 0.404
	0.30	8.002 ± 0.670
	0.35	8.377 ± 0.459
	0.40	9.554 ± 1.237
	0.45	11.450 ± 0.805
	0.50	13.630 ± 0.512
Syn. HA	0.10	5.935 ± 0.321
	0.20	6.674 ± 0.504
	0.35	7.042 ± 0.288
	0.40	8.442 ± 0.647
	0.50	9.990 ± 0.562

The variation of microhardness with volume fraction of filler for the polyethylene composites is shown in Fig.4.1.12.

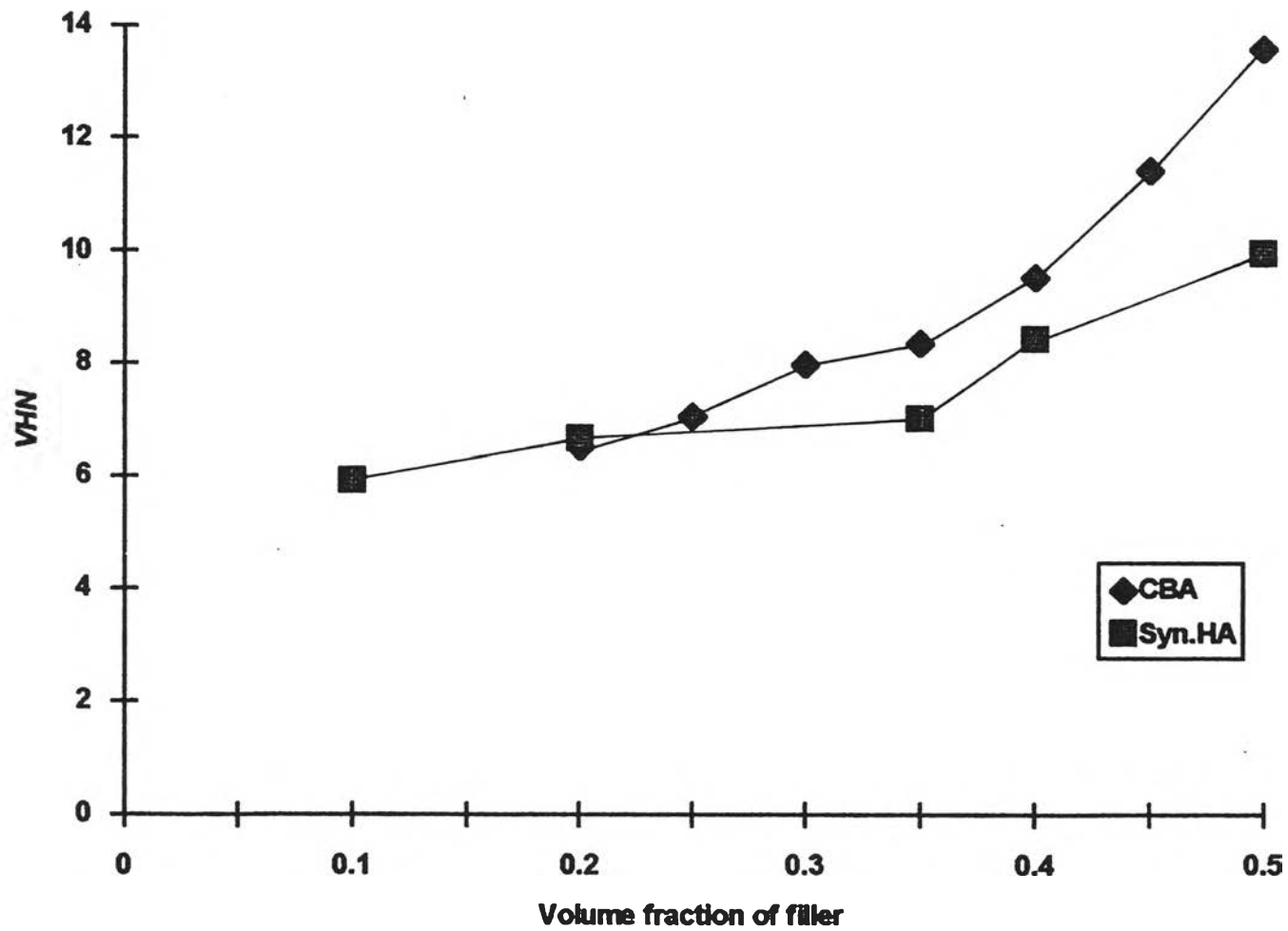


Figure 4.1.12 Variation of microhardness with volume fraction of filler.

## Density Results

The densities of the composites are shown in Table 4.2.1

Table 4.2.1 Density measurement results of calcined bone ash and synthetic hydroxyapatite reinforced high density polyethylene composites at 23°C.

Kinds	Volume fraction of filler	Density (Kg m <sup>-3</sup> )	
		Calculated	Measured
HDPE	0	945	943.1 ± 2.3
CBA	0.10	1166	1056.9 ± 0.6
	0.20	1388	1312.4 ± 8.5
	0.25	1498	1431.5 ± 1.4
	0.30	1609	1596.5 ± 1.7
	0.35	1720	1660.1 ± 1.7
Syn. HA	0.10	1166	1123.1 ± 1.4
	0.20	1387	1315.0 ± 9.1
	0.35	1718	1527.8 ± 18.3

The results show that the value of calcined bone ash reinforced polyethylene composite is closer to the calculated data for the same volume fraction.

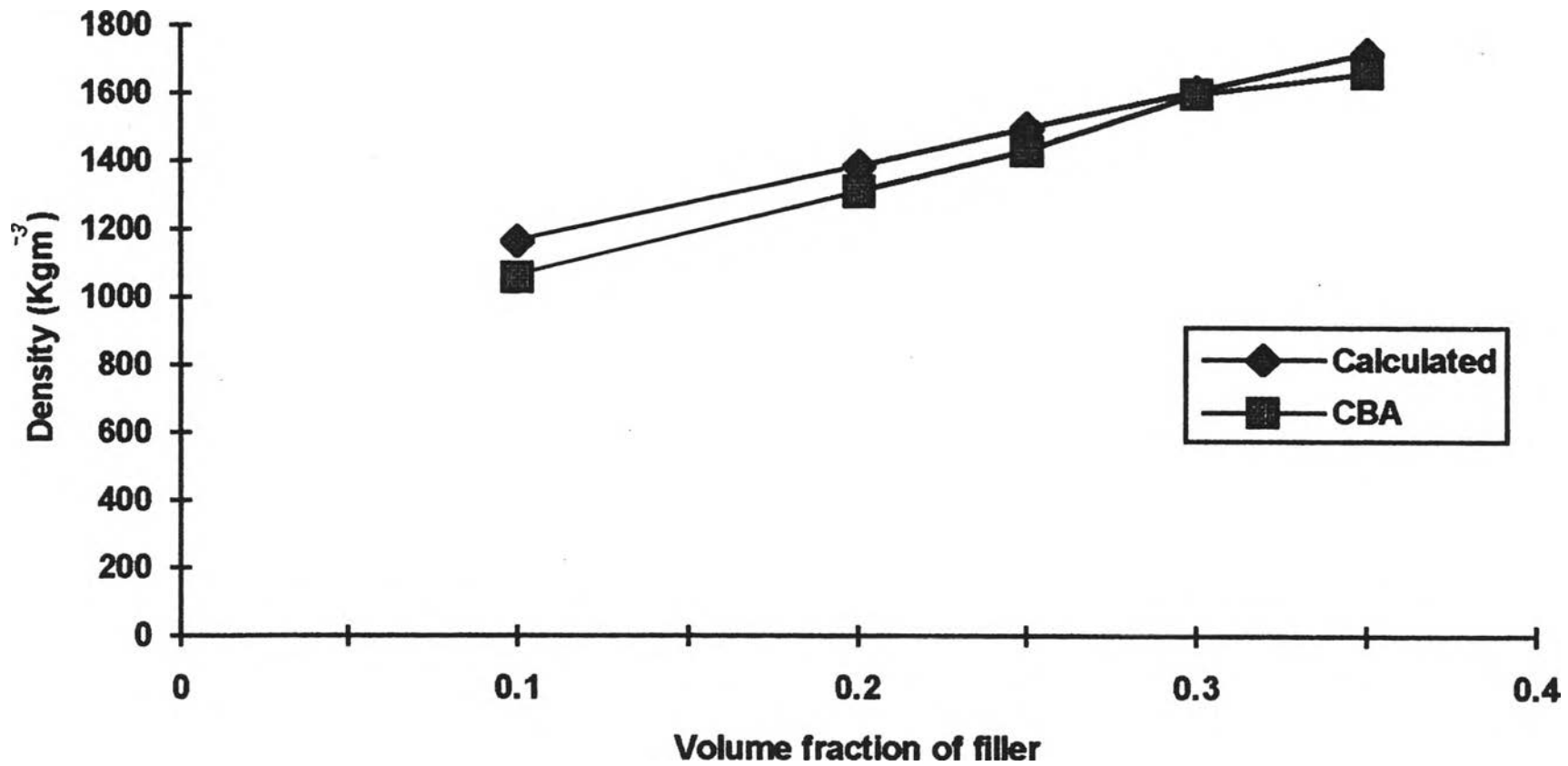


Figure 4.2.1 Comparison of calculated and measured densities of calcined bone ash reinforced polyethylene composites at various volume fraction.

## Dispersion of Filler

Fig.4.3.1 and 4.3.2 shows the scanning electron micrographs of calcined bone ash reinforced polyethylene after polishing and etching. The micrographs confirms a good filler dispersion without agglomerates. Filler particle size distribution is clearly visible.

## Fractography

SEM micrographs were taken of the fracture obtained from tensile tested specimens. They are shown in Fig.4.4.1 to 4.4.7 for varying magnification. They all form little extensive necks, with strainwhitening, before breaking. It can be seen that the hydroxyapatite did not fracture during testing because the ground surfaces of these particles can be seen. Also the separation between the particles and the matrix can be noticed. Fig.4.4.8 show the fracture surface of flexural test. Only one type of the composite was tested because other specimens did not break. This contained 0.45 volume fraction of calcined bone ash and fractured in a more brittle manner than lower volume fractions. The fracture surfaces appear flat, when compared to those of the tensile tested specimens, because polyethylene matrix has been a little drawn out from the composites.

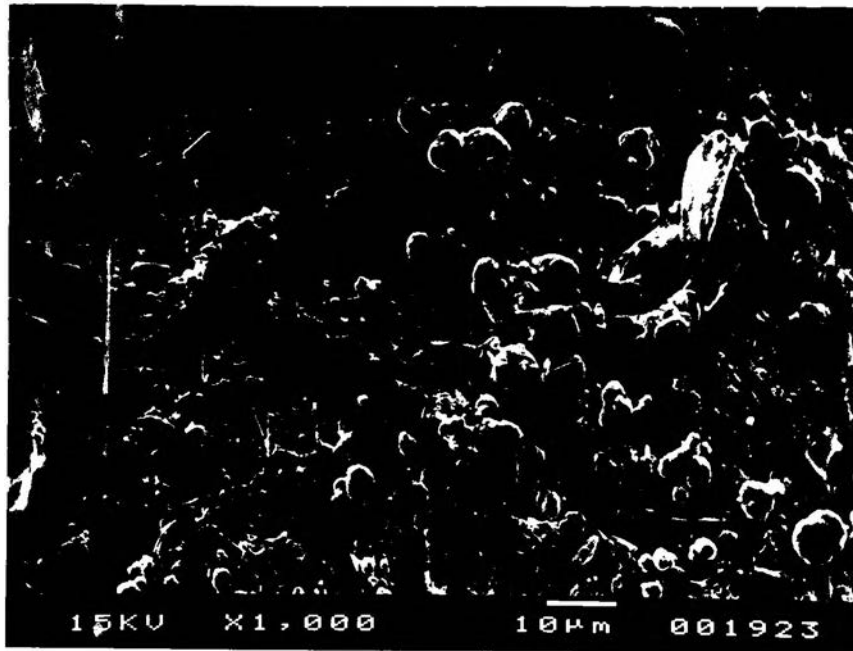


Figure 4.3.1 SEM observation of 0.20 calcined bone ash reinforced polyethylene.

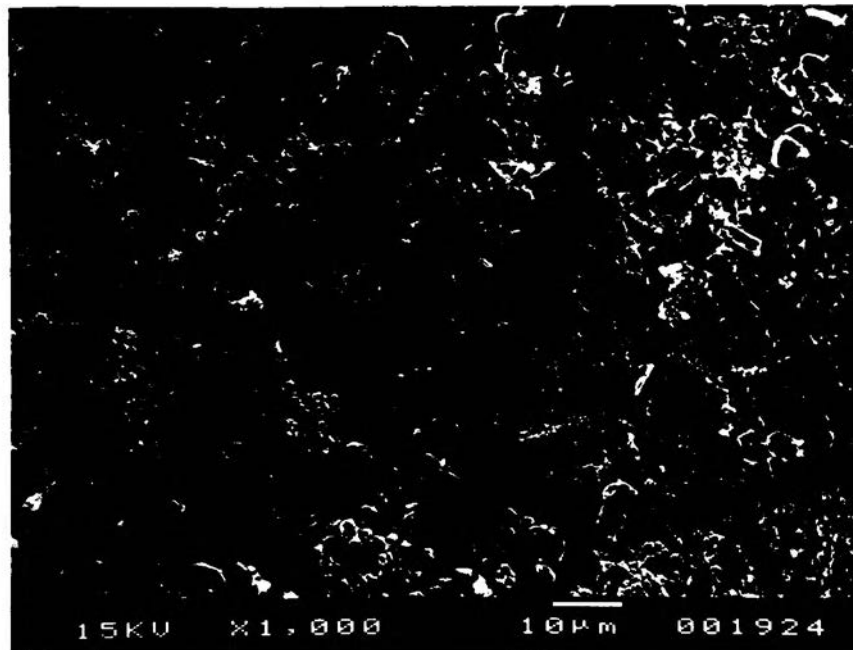
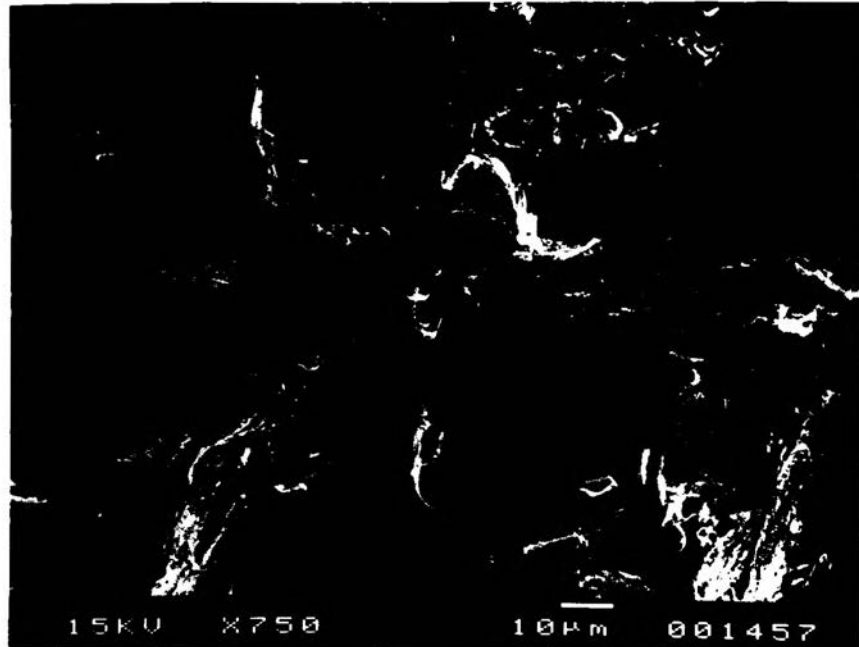


Figure 4.3.2 SEM observation of 0.30 calcined bone ash reinforced polyethylene.



**Figure 4.4.1** Scanning electron micrograph of fracture surface of tensile specimens for 0.20 calcined bone ash volume fraction.



**Figure 4.4.2** Scanning electron micrograph of fracture surface of tensile specimens for 0.30 calcined bone ash volume fraction.



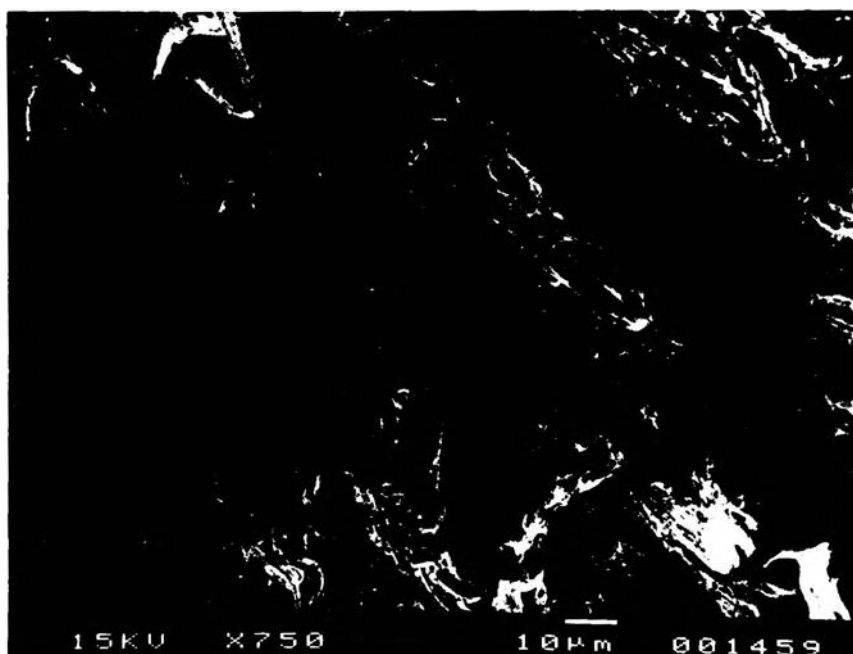
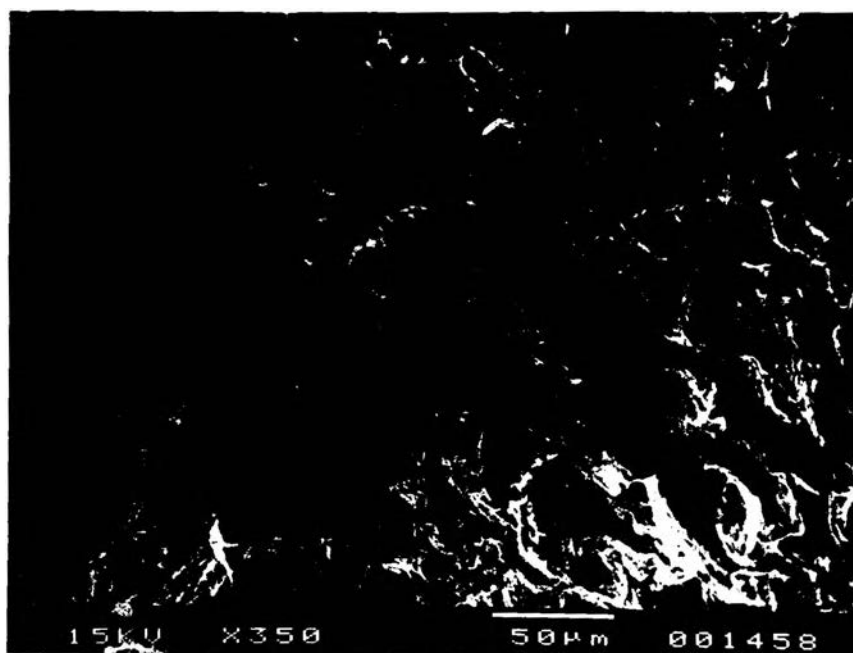


Figure 4.4.3 Scanning electron micrograph of fracture surface of tensile specimens for 0.35 calcined bone ash volume fraction.

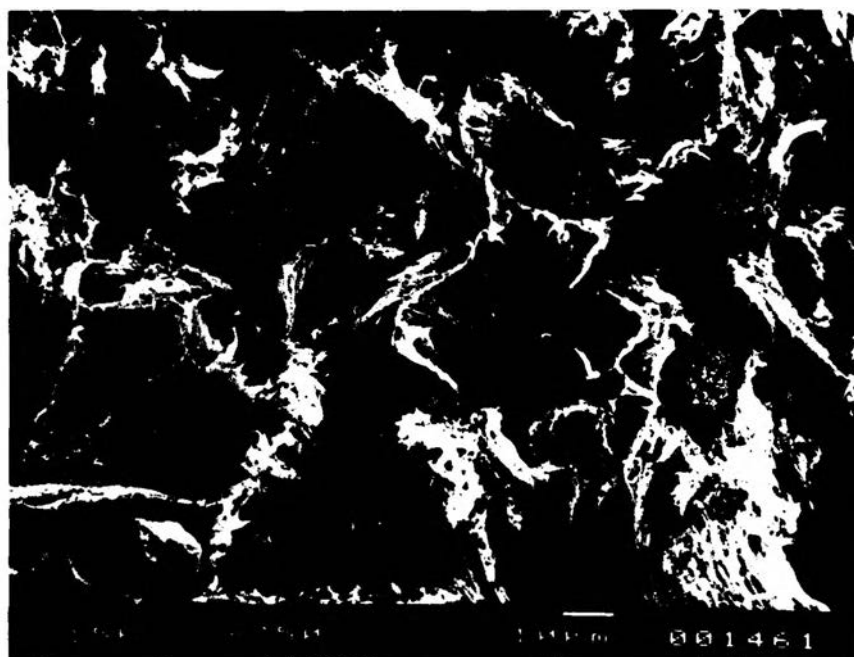
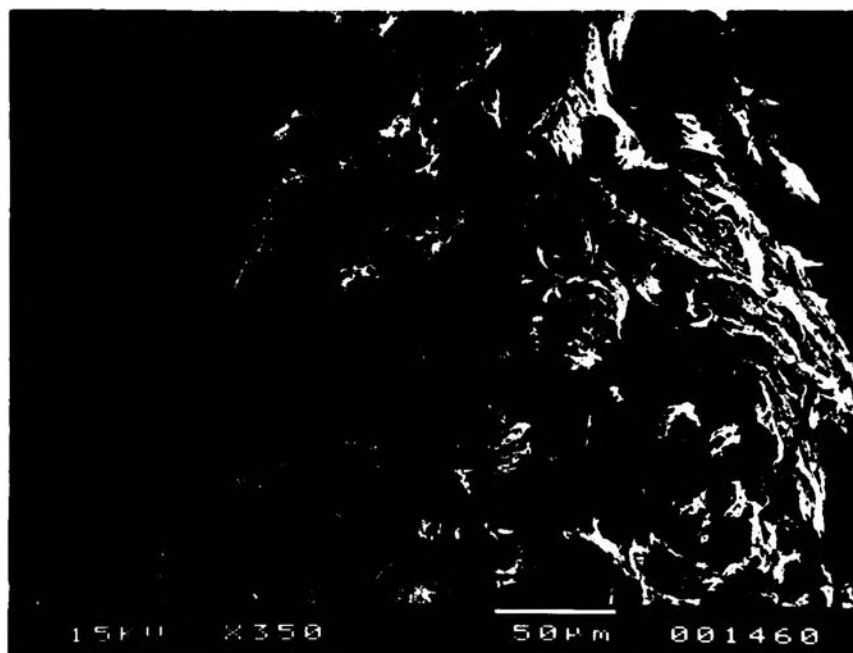
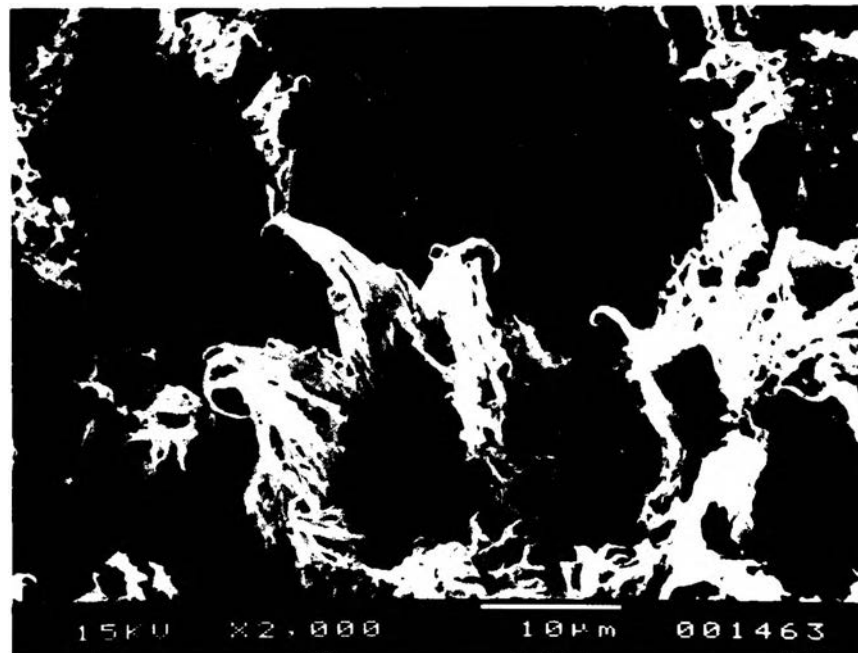
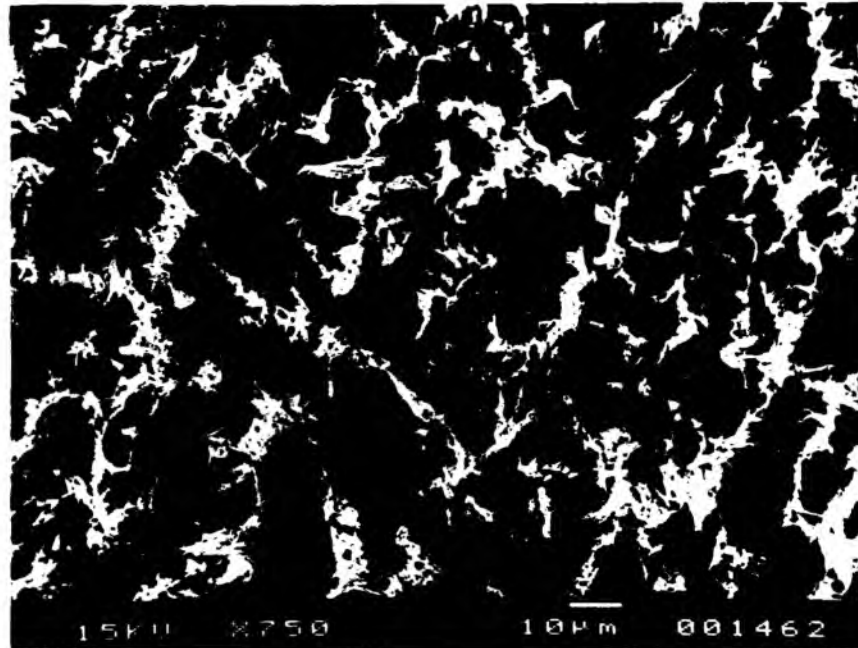
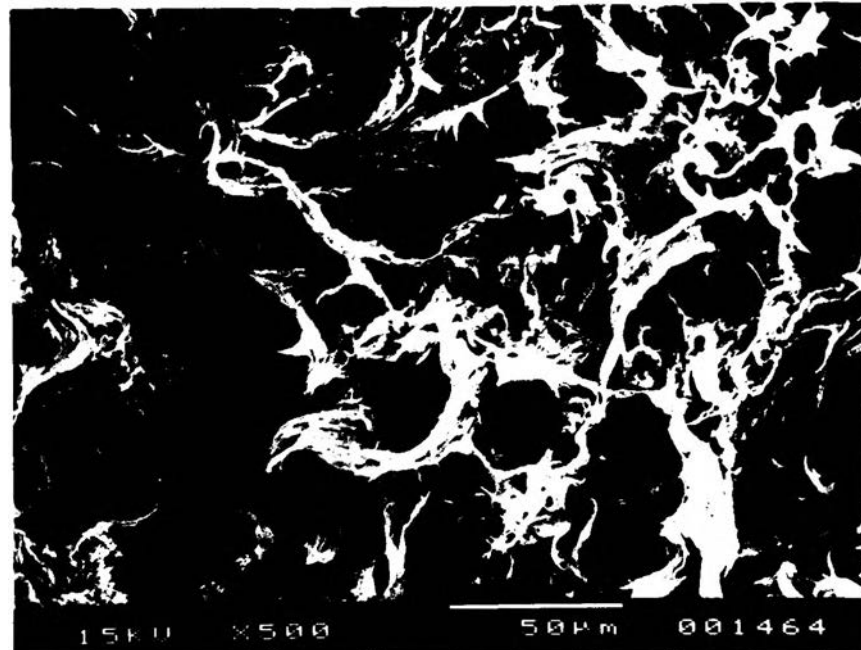


Figure 4.4.4 Scanning electron micrograph of fracture surface of tensile specimens for 0.45 calcined bone ash volume fraction.



**Figure 4.4.5** Scanning electron micrograph of fracture surface of tensile specimens for 0.50 calcined bone ash volume fraction.



**Figure 4.4.6** Scanning electron micrograph of fracture surface of tensile specimens for 0.20 synthetic hydroxyapatite volume fraction.

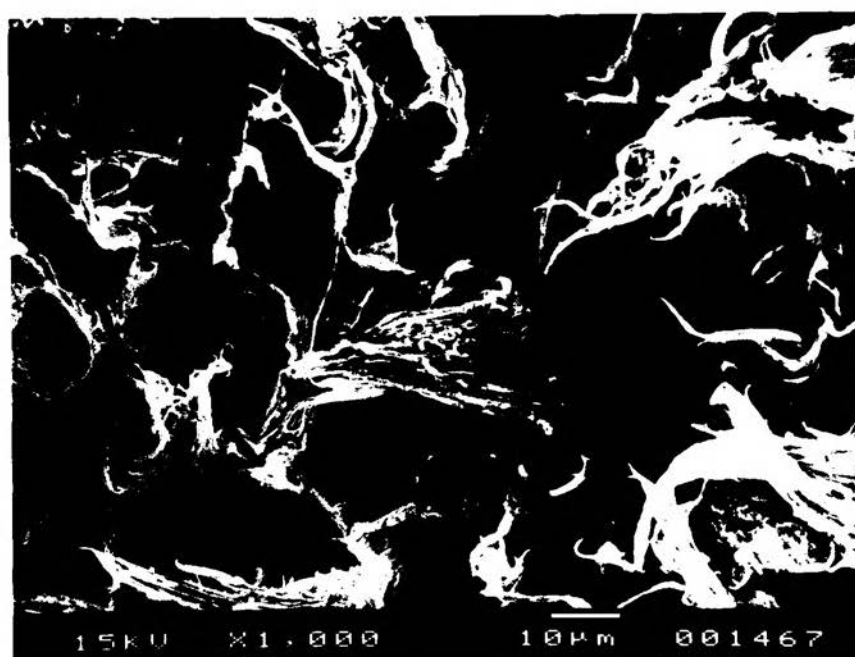
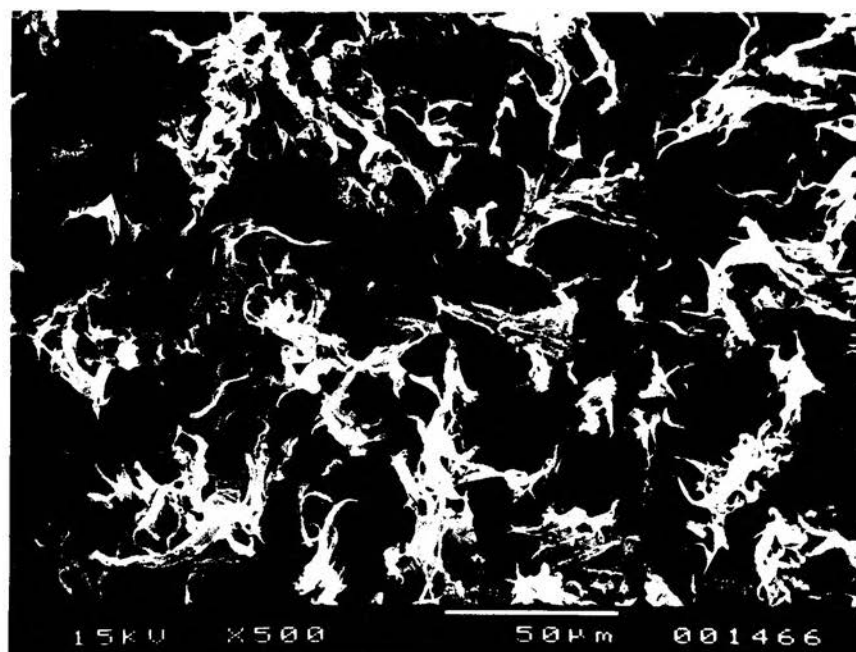


Figure 4.4.7 Scanning electron micrograph of fracture surface of tensile specimens for 0.35 synthetic hydroxyapatite volume fraction.

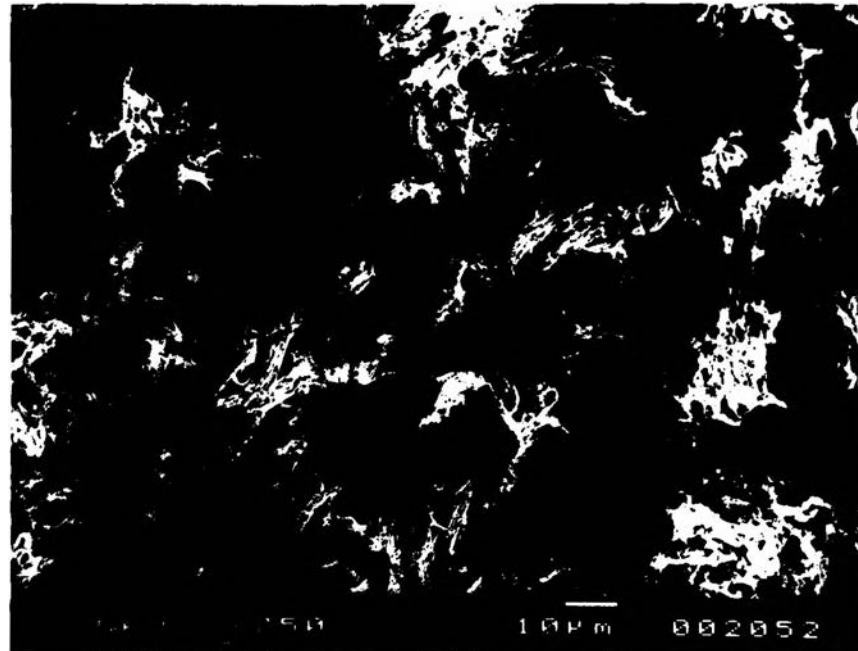
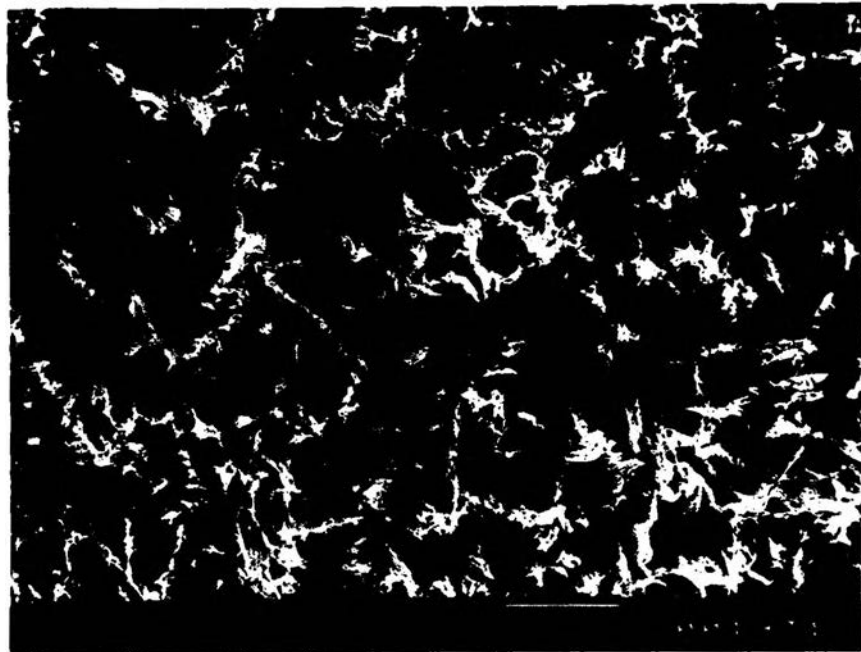


Figure 4.4.8 Scanning electron micrograph of fracture surface of flexural specimen for 0.45 calcined bone ash volume fraction.